Using Microfluidic Chambers to Evaluate the Effect of MitoQ on FUS-mediated Neurotoxicity

Emily Ling

Illinois Mathematics and Science Academy

Mentors: Dr. Jane Wu, Professor of Neurology and Psychiatry; Mengmeng Chen

Feinberg School of Medicine at Northwestern University

Abstract

The purpose of this investigation was to study MitoQ, a mitochondria-targeted antioxidant, as a potential treatment for amyotrophic lateral sclerosis (ALS) and other neurodegenerative diseases associated with mutations in the RNA-binding protein, Fused in sarcoma/Translated in liposarcoma (FUS). Cortical neurons were isolated from day 18 rat embryos and transfected with control, wild-type FUS, and P525L mutant FUS plasmids. Neurons were plated in microfluidic chambers, which are specially-designed devices that use microgrooves to organize axon growth. They were then treated with 0.1 µM, 0.3 µM, or 0.5 µM MitoQ, or the control. The neurons were fixed and stained after one week, and were imaged using a fluorescent microscope. 0.3 µM and 0.5 µM MitoQ treatments were toxic, so only the control and 0.1 µM MitoQ treatments were analyzed. Mitochondrial fragmentation, dendrite length, and branch point number were observed and quantified. The results showed that FUS transfections significantly worsened mitochondrial fragmentation, as expected ($p<0.0001$). However, MitoQ treatment significantly worsened all three aspects of neuronal health ($p<0.05$). This unexpected result is likely due to toxic byproducts in the MitoQ, which may not have been sufficiently purified during production. Despite these results, MitoQ may still be a promising therapy for ALS, and further investigation is suggested.

Focusing Question

How does Fused in sarcoma/Translated in liposarcoma (FUS) protein affect mitochondrial and neuronal health in amyotrophic lateral sclerosis (ALS), and is MitoQ an effective drug in reducing the neurotoxicity?

Introduction

Neurodegenerative diseases are a group of progressive disorders that affect the nervous system and cause irreversible deterioration in motor skills, behavior, and/or cognitive function (Chaturvedi & Flint Beal, 2013). One such neurodegenerative disease is amyotrophic lateral sclerosis (ALS), which is an adult-onset disease that is characterized by the degeneration and death of motor neurons. Thus, ALS patients suffer from impaired motor abilities and gradually experience muscle weakness and paralysis. ALS is typically fatal within two to five years after diagnosis due to respiratory failure and/or paralysis (Al-Chalabi et al., 2012; Couthouis et al., 2012; Lagier-Tourenne & Cleveland, 2009). Approximately 10 percent of ALS cases are hereditary, while the remaining 90% of cases occur sporadically without any family history of the disease (Ugras & Shorter, 2012). Although the exact cause of the disease is unknown, researchers have identified several proteins that are often overexpressed and/or mutated in both familial and sporadic ALS. One such protein is the Fused in sarcoma/Translated in liposarcoma (FUS/TLS, FUS) protein (Couthouis et al., 2012; Lagier-Tourenne & Cleveland, 2009).

FUS is a nuclear RNA-binding protein that is encoded by the FUS/TLS gene. This protein plays a significant role in DNA repair, splicing, and transcription. It is also involved in miRNA processing and mRNA transport (Blokhuis, Groen, Koppers, Berg, & Pasterkamp, 2013; Lagier-Tourenne & Cleveland, 2009). It is yet unclear if FUS proteinopathy is caused by a loss of function or gain of function toxicity, but these two mechanisms are not necessarily mutually exclusive (Armstrong & Drapeau, 2013; Murakami et al., 2012). Over 50 different reoccurring mutations have been identified on the FUS/TLS gene among ALS and frontotemporal lobar degeneration (FTLD) patients (Da Cruz & Cleveland, 2011). One such ALS-linked mutation, Pro-525-Leu (P525L), is a missense mutation created when proline is exchanged for leucine at

the 525th position of the FUS/TLS gene (See Figure 1). This mutation is associated with severe juvenile and familial ALS, and has been shown to cause cytoplasmic mislocalisation and other severe disruptions in cellular function (Conte et al., 2012; Dormann et al., 2010; Murakami et al., 2012).

Models of FUS proteinopathies have recapitulated many of the key features and symptoms of ALS. In a yeast model of FUS-mediated ALS, cells demonstrate protein aggregation and cytotoxicity similar to that found in ALS patients (Fushimi et al., 2011). Drosophila flies expressing either wild-type and mutant FUS proteins in the motor neurons or mushroom bodies demonstrate progressive degeneration, axon loss, and cell death (Chen et al., 2011). Several other models of FUS-mediated ALS have shown similar results (Armstrong & Drapeau, 2013; Lanson et al., 2011; Murakami et al., 2012; Xia et al., 2012). FUS proteinopathy has also been linked to mitochondrial damage and dysfunction. In one study, expression of ALS-linked FUS mutants in neuronal cells was shown to lead to mitochondrial fragmentation (Tradewell et al., 2012). Mitochondria dysfunction, particularly relating to oxidative stress, axonal transport, apoptosis, and excitotoxicity, is believed to be a fundamental contributor to ALS. Mitochondria play an essential role in motor neuron survival, energy production, and regulation of apoptosis, all of which are large factors in ALS (Cozzolino & Carrì, 2012; Manfredi & Xu, 2005; Shi, Gal, Kwinter, Liu, & Zhu, 2010). In a broader sense, there is growing evidence that mitochondria play a central role in many neurodegenerative diseases. Thus, mitochondria-targeted drug therapies hold great promise for patients (Lin & Beal, 2006).

A major method used in neuroscience research is neuronal cell culture, which involves the controlled growth of neurons in a laboratory setting. This method is widely used to study the basic structure, development, and properties of neurons, as well as to screen various drugs and

chemicals in neuronal models of disease (Giordano & Costa, 2011). Neurons, which are the fundamental building blocks of the nervous system, function to receive and transmit signals to and from other parts of the body or brain. The four main regions of a neuron are the cell body, dendrites, axon, and axon terminals. The cell body, which contains the nucleus, synthesizes the majority of the cell's proteins and membranes. The cell body transmits signals through the axon, which is an extension of the cell. An axon only carries signals away from the cell body, and these signals are transmitted in the form of a cascade of sudden changes in the voltage across the plasma membrane, known as an action potential. The action potential continues to travel along the axon until it reaches the axon terminals. The axon terminal is the point at which a cell forms a synapse with the dendrite of the next neuron. Neurotransmitters then pass the signal across the synapse, where it is transmitted by the dendrite to the cell body. The cell body integrates the signals it receives from the dendrites, and then it can pass another signal along its axon. (Lodish, Berk, & Zipursky, 2000).

During neuronal development, axons grow over very long distances, forming synapses whenever other neurons are encountered. Over time, as the organism develops, improper or redundant connections are sculpted away in order to increase signal transduction efficiency (Colon-Ramos, 2009). However, this method of neuronal development makes for very difficult data analysis in laboratory neuronal culture. When left to grow normally, neurons form connections with countless other neurons, creating a highly complex neural net. If a picture of cultured neurons is isolated from the original sample, it becomes nearly impossible for a researcher to determine the origin of a specific axon or dendrite, quantify damage, or measure the length of an axon or dendrite, making data analysis very difficult. However, microfluidic chambers offer an innovative new method for neuronal culture. Microfluidic chambers are small

devices that allow the researcher to precisely control the development and growth environment of neurons. This results in neurons that grow in a highly organized manner. Despite their small size, microfluidic chambers can also produce large quantities of data, making them a highly efficient device (Cohen, Orth, Kim, Jeon, & Jaffrey, 2011; Wang et al., 2009).

The microfluidic chambers used in this investigation were specifically designed to produce highly organized results. The chamber is 14 mm in diameter, which is small enough to place into one well of a 12-well microtiter plate. It is made from polydimethylsiloxane (PDMS), and each chamber contains 500 microgrooves which are deep enough for only axons and dendrites to pass through. By separating the cell bodies from the neurites, the microgrooves allow for easy analysis. Additionally, axons and dendrites are forced to grow in straight lines through the microgrooves, preventing them from forming a complex net. Each microfluidic chamber can hold approximately 15,000 neurons, providing a large quantity of data in a very small device. Thus, microfluidic chambers not only improve the accuracy and ease of data analysis, but they are also highly efficient and convenient (See Figures 2 and 3).

Microfluidic chambers provide a powerful platform on which to screen various drugs and compounds. Using a neuronal model of FUS-mediated ALS, this investigation will test the drug MitoQ. MitoQ is an antioxidant that consists of the covalent attachment of ubiquinone to a triphenylphosphonium lipophilic (TPP) cation (Kelso et al., 2001). Ubiquinone is the oxidized form of coenzyme Q10 (CoQ10), which is an antioxidant as well as part of the electron transport chain in the mitochondria. Because CoQ10 plays such an important role in cellular energy production, it may assist with motor function and thus be a potential drug for ALS (Hargreaves, 2003). However, because ubiquinone is fat-soluble, it is difficult for cells to absorb and utilize the compound on its own. This problem can be overcome through the covalent attachment of

ubiquinone to a TPP cation. TPP cations, which have a positive charge, accumulate in high concentrations in the mitochondria. They can also pass easily through the blood-brain barrier and into muscle cells to where they are needed most. Thus, the conjugation of ubiquinone to a TPP cation not only makes the drug more accessible to cells, but it also specifically targets the mitochondria where the ubiquinone is most effective (Murphy & Smith, 2007). MitoQ has previously been shown to have antioxidant and antiapoptotic properties in cells (Kelso et al., 2001). It has shown promise in models of both Parkinson's disease and Alzheimer's disease (McManus, Murphy, & Franklin, 2011; Tauskela, 2007). Because ALS, particularly FUS-mediated ALS, is associated with mitochondrial dysfunction, MitoQ may also be an effective treatment for ALS patients. This investigation will determine the effect of MitoQ treatment on a neuronal model of FUS-mediated ALS.

Materials and Methods

General Cell Culture Techniques:

All procedures involving live cells were performed under the hood in order to minimize the risk of bacterial infection. All materials, including gloved hands, were sanitized with ethanol spray before entering the hood. Any biologically hazardous waste, including any materials that came into contact with cells, was placed in a biohazard bag and was properly disposed. When the hood was not in use, the UV light was turned on in order to kill bacteria.

Non-neuronal cells were cultured in normal DMEM growth medium. This consisted of DMEM with 10% fetal bovine serum (FBS) and 0.5% penicillin/streptomycin for anti-bacterial purposes. Neuronal cells were cultured in neurobasal growth medium, which consisted of 2% B27 supplement, 0.5 mM glutamine, and 1% penicillin/streptomycin.

Primary Cortical Neuron Culture:

The protocol for primary cortical neuron culture involves dissecting the cortexes of E18 rat embryos in order to grow these neurons for experimental purposes. All the neurons tested in this investigation came from this protocol.

1. Euthanize one pregnant rat with day 18 fetuses by CO2 asphyxiation followed by thoracotomy.
2. Cut into the rat on the lower part of the abdomen using scissors. Cut open the uterus and remove the fetuses, cutting the connective tissue as you go. Place the fetuses in a petri dish on ice.
3. Cut open the membranes surrounding the embryos in order to expose the embryos.

4. Using forceps, cut off the head of each embryo. Hold the embryo near the mouth with the top of the head facing upwards. Using curved forceps, make a slit in the center of the skull from the front to back, cutting through both the scalp and the skull.
5. Remove the brain using curved forceps by scooping out the brain, and place it in a Petri dish containing ice-cold medium.
6. Placing the brain face-up, use forceps to roll out and cut off the cortex from each hemisphere.
7. Put all dissected cortexes together and mince with forceps. Transfer the tissues to a 15 ml tube containing 4 ml of papain solution. Incubate at 37^{o}C for 15 minutes.
8. Add 2 ml neurobasal medium, and gently pipette the tissues up and down.
9. Allow the solution to settle for 30 seconds, and then transfer 2 ml of supernatant into a new 15 ml tube. Repeat this step 3 times, adding more neurobasal medium as necessary. If the remaining solution contains no visible tissue pieces, transfer the rest of the solution to the tube.
10. Spin cell suspension for 2 minutes.
11. Remove supernatant, and resuspend cell pellet in 6 ml neurobasal medium.
12. Filter cell suspension through a cell strainer into a 50 ml tube.
13. Mix 5 µl cell suspension, 50 µl trypan blue dye, and 45 µl neurobasal medium in an Eppendorf tube. Count viable cells to determine the cell density.
14. Dilute cell suspension to the desired density for plating. The density used for the microfluidic chambers is $5*10^{6}$ cells/ml.

Electrotransfection:

The neurons that would be treated with MitoQ were transfected using an electrotransfection machine. The protocol for electrotransfection is as follows:

1. Transfer 4 µg of DNA to each Eppendorf tube.
2. For each tube of DNA that will be used, transfer $5*10^6$cells into a 15 ml tube. Spin down cells in the centrifuge.
3. Resuspend the cell pellet in Solution I+II, 100 µl for each tube of DNA that will be used.
4. Add 100 µl of the cell solution to each tube of DNA.
5. Pipette up and down to mix, then immediately pipette the mixture into the electrotransfection chamber.
6. Place the chamber in the electrotransfection machine and press the button.
7. Immediately add 1 ml neurobasal medium to the chamber to stop cell damage.
8. Repeat steps 4-6 with each tube.
9. Remove cells from the electrotransfection chamber and plate normally.

Neurons were transfected with control, wild-type FUS, and P525L mutant FUS plasmids. The protocol is performed on neurons harvested from primary cortical neuron culture on the same day. These neurons were then plated into chambers and treated with MitoQ. Two cover slips were prepared for each combination of plasmid and MitoQ treatment. The cells were allowed to grow for one week before being fixed and stained.

Lipofectamine2000 Transfection:

A Lipofectamine2000 transfection was performed to confirm the mitochondrial damage and neurotoxicity caused by FUS protein. The transfection was performed on neurons that had

been harvested two weeks earlier and grown on cover slips with normal neurobasal growth medium without a microfluidic chamber.

1. Add 100 µl of HEPES to 10 mL DMEM, and warm the mixture to 37 ^{o}C. This is known as h-DMEM.
2. Transfer cover slips to new wells containing 600µL neurobasal medium without penicillin/streptomycin. Save the old medium in a 15 ml tube.
3. Incubate cells for 30 minutes at 37 ^{o}C.
4. For each cover slip being transfected, add 50 µL of h-DMEM and 3 g of DNA to an Eppendorf tube.
5. In a larger tube, mix 50 µL of h-DMEM and 3 µL of LFA2K for each cover slip.
6. Allow the mixtures to rest at room temperature for 5 minutes.
7. Add 50 µL of the LFA2K mix to each tube of h-DMEM+DNA.
8. Pipette up and down to mix for each tube.
9. Incubate for 20 minutes at 37^{o}C with caps open.
10. Add the mixture drop by drop to the wells with the cover slips.
11. Incubate at 37^{o}C for at least 4 hours.
12. Replace the cover slips into the old wells with half the original medium and half fresh medium.

Control, wild-type FUS, and P525L mutant FUS plasmids were used in this transfection. The cells continued to grow for 3 days before being fixed.

<u>Microfluidic Chamber Set-up:</u>

The microfluidic chambers were cut out from a piece of polydimethylsiloxane (PDMS) which were engraved with the microgrooves. Two large holes were punched in the areas

connected by the microgrooves, and two smaller holes were punched on the sides of the microgrooves. The chambers were then cut out and shaped into octagons using a blade.

Prior to use, both the chambers and glass cover slips, which are used for plating, were thoroughly cleaned. The microfluidic chambers are reused between experiments. After being removed from the cover slips, the chambers were rinsed under running water, focusing on the side with microgrooves. The chambers were then placed in an ultrasonic washing machine filled with detergent solution for 2 hours, and were stirred every 30 minutes to separate the chambers. The detergent water was removed, and the chambers were incubated in water for 1 hour. Each chamber was then rinsed again in running water, which was followed by an overnight soak in 70% ethanol. The chambers were then placed in glass Petri dishes and autoclaved for 30 minutes.

To wash the glass cover slips, the cover slips were first placed in large glass Petri dishes and soaked in 1 M hydrochloric acid (HCl) overnight. The following day, they were washed three times in 70% ethanol and one time in 100% ethanol for one hour each. The petri dishes were then wrapped in aluminum foil and autoclaved for 30 minutes. After drying, the cover slips were transferred to sterile 12-well plates and coated with poly-D-lysine (PDL) overnight, which enhances cell adhesion to the cover slips. The next day, the cover slips were washed 3 times with autoclaved water under the hood, and were left to dry in the plates overnight.

To set up the chambers for plating, the microfluidic chambers were placed with the microgrooves facing down on the cover slips already in 12-well plates. The chamber must be placed firmly on the cover slip to seal the edges of the chamber. After preparing the primary neuron culture, 5 µl of cell solution was pipetted into each of the two large holes. The chambers were incubated for 15 minutes at 37^{o}C. The two large holes were then filled with neurobasal

growth medium containing 10% fetal bovine serum. After 1-3 days, a third hole was filled with neurobasal medium. The neurons were kept in an incubator at 37^{o}C until fixing and staining.

MitoQ Treatment:

Neurons were treated with MitoQ at concentrations of 0.1 µM, 0.3 µM, and 0.5 µM. The control was standard neurobasal growth medium with 10% fetal bovine serum. The MitoQ solutions were added to the chambers after the neurons had been plated.

Fixing, staining, and mounting:

When the neurons were ready to be fixed, the chambers were carefully removed using forceps so that the neurons were left on the cover slip. These neurons were then fixed and stained with antibodies for further study, using this protocol.

1. Remove media from plates, wash cells with 1x PBS for 5 minutes.
2. Fix the cells with 4% paraformaldehyde (PFA) in 1x PBS at room temperature for 20 minutes (or overnight at 4^{o}C). Optional: Wash with methanol for 15 minutes at -20^{o}C.
3. Wash the cells 3 times with 1x PBS for 5 minutes each.
4. Wash the cells with 0.5% TritonX100 at room temperature for 10 minutes.
5. Block and permealize the cells with block solution (5% NGS or 3% BSA) at room temperature for 1 hour.
6. Add primary antibodies (Diluted 1:500 or adjust based on strength, in block solution). Store in the dark, overnight at 4^{o}C or at 37^{o}C for 2 hours.
7. Wash the cells 3 times with wash solution at room temperature for 5 minutes each.
8. Add secondary antibody (1:500 dilution in block solution) and Hoechst dye (1:1000 dilution in block solution). Incubate for 1 hour at room temperature, in the dark.
9. Wash the cells 3 times with wash solution in the dark, 5 minutes each.

10. Mount the cover slips with mount solution and allow to dry in a dark place for 24 hours. The cells are now ready for observation.

The FUS transfection cells were stained with anti-GFP and anti-bassoon first antibodies, with Cy2 and Alexa 555 secondary antibodies, as well as Hoechst dye. The MitoQ-treated cells were stained with anti-RFP and anti-Tuj1 first antibodies, Alexa 555 and Alexa 488 secondary antibodies, and Hoechst dye.

Microscope imaging:

The neurons were imaged using a fluorescent microscope. The 63x oil-immersion lens was used, and cells were imaged using the FITC channel (green, for Cy2 or Alexa 488 staining), DAPI channel (blue, for Hoechst dye), and Cy3 channel (red, for Alexa 555 staining). Z-stack images were taken with the focus at the center, with 7 images each 1 μm apart. The images were then combined by creating an image with extended depth of field.

Results

The 0.3 µM and 0.5 µM MitoQ treatments created toxic effects, causing neuronal death. Thus, the neurons receiving these treatments were not analyzed for results. The neurons treated with 0.1 µM MitoQ and no MitoQ were analyzed for mitochondrial fragmentation percentage, dendrite length, and the number of branch points per neuron. Images were taken using a fluorescent microscope, and were taken separately for mitochondria and dendrite analysis. Images depicting mitochondria can be found in figure 4, and images depicting dendrites can be found in figure 5 in the appendix.

Mitochondrial fragmentation percentage was evaluated for each 30 µm segment of each dendrite, based on the percentage of length not covered by mitochondria. The data was graphed with error bars with one standard error above and below the mean (Figure 6). To analyze the data, a two-way ANOVA test and two-sample t-tests with F-tests for variance were performed. The control, wild-type FUS, and P525L mutant FUS transfections were found to be significantly different ($p<.0001$). More specifically, the control transfection had significantly lower mitochondrial fragmentation, at 40.64% fragmentation, than both the wild-type FUS transfection at 46.4% ($p=0.0178$) and the P525L mutant FUS transfection at 54.77% ($p<.0001$). Additionally, 0.1 µM MitoQ treatment significantly worsened the mitochondrial fragmentation ($p=0.0013$). In the control transfection, MitoQ treatment significantly increased the mitochondrial fragmentation from 40.64% to 50.86% ($p=0.047$).

Dendrite length was measured from the cell body to the end of the dendrite. Each dendrite was measured separately, and the resulting dendrite from each branch point was also measured separately. The data was graphed with error bars one standard error above and below the mean, and this graph can be found in figure 7 in the appendix. A two-way ANOVA test and

two-sample t-tests with F-tests for variance were performed. There was found to be no significant difference between the three transfections ($p=0.134$). However, the P525L transfection had a significantly lower average dendrite length of 55.944 μm, than did the control transfection at 67.202 μm ($p=0.0008$). The 0.1 μM MitoQ treatment was found to significantly decrease the dendrite length ($p=0.0036$). Specifically, in the control transfection, MitoQ treatment decreased the mean dendrite length from 67.202 μm to 51.406 μm ($p=0.0096$).

The number of branch points was counted for each neuron. A branch point was defined as a point at which a single dendrite split into two dendrites. The average number of branch points per neuron was graphed with error bars depicting one standard error above and below (Figure 8). Again, a two-way ANOVA test and two-sample t-tests with F-tests for variance were performed. Although there was no significant difference between the three transfections, there was a significant difference between the neurons treated with 0.1 μM MitoQ and those that were not. 0.1 μM MitoQ significantly decreased the number of branch points per neuron ($p=0.0302$).

Images were also taken of the axons that had grown into the microgrooves of the microfluidic chambers, using the FITC channel. These images were not quantified, but they were observed qualitatively. The images can be found in figure 9 in the appendix. The wild-type FUS and P525L mutant FUS transfections caused greater axon fragmentation and reduced the width and quantity of axons. Treatment with 0.1 μM MitoQ caused more severe fragmentation, thinning, and disorganization of axons.

Conclusion

Although this investigation initially set out to test three different concentrations of MitoQ, all but the lowest concentration caused neuron death. Very few or no neurons were able to survive when treated with either 0.3 μM or 0.5 μM MitoQ, suggesting that higher concentrations of MitoQ are toxic to neurons. Thus, the investigation only yielded results for 0.1 μM MitoQ and the control treatment.

Prior to experimentation, the effects of FUS transfection were also tested. Neurons were transfected with control, wild-type FUS, and P525L mutant FUS plasmids and grown normally on cover slips. This initial test showed that both the wild-type FUS and P525L mutant FUS transfections caused neuronal damage, including signs such as reduced dendrite length, thinning of axons, and fragmentation. These negative effects were further magnified in the P525L mutant FUS transfection, suggesting that the ALS-linked FUS mutations cause increased toxicity. This initial small experiment was performed to confirm the neurotoxicity of FUS, and the results confirmed the researcher's expectations.

The dendrites and mitochondria were analyzed separately in order to examine multiple aspects of neuron health. The most conclusive results came from the mitochondrial fragmentation data. The data once again confirmed that FUS expression, particularly the P525L mutant FUS, has negative effects on neuronal health. In particular, FUS transfection significantly worsened mitochondrial damage, suggesting that FUS proteins impact mitochondrial health. Additionally, mitochondrial fragmentation significantly increased with MitoQ treatment, suggesting that MitoQ actually had toxic effects on the neurons. This trend was true for all three transfections, even for the control.

The toxicity of MitoQ was further suggested by the dendrite analysis data. The results from the dendrite length measurements showed that MitoQ significantly decreased the average dendrite length. Healthier neurons tend to have longer-reaching dendrites in order to form wide-ranging, effective connections; thus, the decrease in average dendrite length suggests that MitoQ negatively impacts neuronal health. Additionally, the dendrite length analysis also showed that the P525L mutant FUS transfection had toxic effects on the neurons. Although the branch point analysis did not show significant differences between the three transfections, it did further confirm the toxicity of MitoQ. Healthier neurons tend to have more branch points, allowing them to form greater numbers of connections. MitoQ treatment significantly decreased the average number of branch points per neuron, showing that MitoQ damaged neuron health.

Finally, qualitative observation of the microgrooves confirmed the results suggested in the previous analyses. The neurons transfected with wild-type or P525L mutant FUS showed axonal damage, and these effects were magnified with MitoQ treatment. MitoQ increased the fragmentation of axons while decreasing the width and quantity of axons, once again suggesting the negative effects of MitoQ.

Discussion

Based on the results, several conclusions can reasonably be drawn. First, both wild-type FUS and P525L mutant FUS protein expression have negative impacts on neuronal health, particularly mitochondrial health. This confirms the prediction that ALS, particularly FUS-mediated ALS, is associated with mitochondrial dysfunction and damage. This result is supported by previous research in the field, which shows that mitochondria play a central role in ALS and other neurodegenerative diseases (Cozzolino & Carrì, 2012; Lin & Beal, 2006; Manfredi & Xu, 2005). The data also showed that the mitochondrial damage and neurotoxicity from FUS are correlated, as both the mitochondrial and dendrite analyses demonstrated the negative effects of FUS. However, it is yet unclear exactly how mitochondrial damage is associated with neurotoxicity and cell death in ALS.

Additionally, the results of this investigation suggest that MitoQ has a significant toxic effect towards neurons. This is highly unexpected and is contrary to the results of several published studies (McManus et al., 2011; Tauskela, 2007). There are several potential explanations for this result. One possible explanation is that the mitochondrial damage found in ALS differs from the type found in Parkinson's disease and other neurodegenerative diseases; thus, MitoQ may not be an effective treatment for ALS. This explanation is unlikely, however, due to the molecular similarities between ALS and other neurodegenerative diseases, as well as the results of previous studies involving MitoQ. A much more likely explanation is that the MitoQ used in this experiment contained byproducts that had been generated as a result of MitoQ production. The MitoQ came from another lab that independently produced the drug, rather than from a pharmaceutical company. Thus, it is highly likely that the drug contained high levels of toxic byproducts that had not been sufficiently purified. This explanation is further

supported by the fact that MitoQ actually caused mitochondrial damage rather than improving it. Because MitoQ was designed to improve mitochondrial function, it is likely that the damage observed was a result of other chemicals.

Although this investigation was not able to conclusively test MitoQ as a potential drug for ALS, it did demonstrate the effectiveness of microfluidic chambers in neuronal culture. Images taken of the microgrooves demonstrated the same results and patterns of damage as did the detailed analysis of the mitochondria and dendrites. The health of the axons in the microgrooves reflected the health of the neurons outside of the chamber, suggesting that the microfluidic chambers do not greatly distort the data. Neurons were able to effectively develop in the chambers, and the microgrooves adequately performed their function in keeping the axons straight and organized, separate from the cell bodies. Thus, in the future, microfluidic chambers could be a highly useful tool in neuronal culture. By screening drugs on cells grown in microfluidic chambers, researchers could obtain large amounts of data in a highly efficient and accurate manner.

Future plans for the investigation include testing a much more purified form of MitoQ, as well as testing other drugs that target oxidative stress, ATP production, and the mitochondria. There is much work that can be done by combining the methods used in this investigation with more emerging, new technology. By demonstrating the effectiveness of these methods, this investigation has helped to improve the tools and techniques available in neuroscience research. For example, an automated axonal damage computer program, which has been recently developed, would be able to quantify axonal damage in the microgrooves in a highly accurate manner, allowing researchers to screen drugs at a much higher rate. These future studies hold great potential for those afflicted with ALS and other neurodegenerative diseases.

References

Al-Chalabi, A., Jones, A., Troakes, C., King, A., Al-Sarraj, S., & van den Berg, L. H. (2012). The genetics and neuropathology of amyotrophic lateral sclerosis. *Acta neuropathologica*, *124*(3), 339–352. doi:10.1007/s00401-012-1022-4

Armstrong, G. A. B., & Drapeau, P. (2013). Loss and gain of FUS function impair neuromuscular synaptic transmission in a genetic model of ALS. *Human molecular genetics*. doi:10.1093/hmg/ddt278

Blokhuis, A. M., Groen, E. J. N., Koppers, M., Berg, L. H., & Pasterkamp, R. J. (2013). Protein aggregation in amyotrophic lateral sclerosis. *Acta Neuropathologica*, *125*(6), 777–794. doi:10.1007/s00401-013-1125-6

Chaturvedi, R. K., & Flint Beal, M. (2013). Mitochondrial Diseases of the Brain. *Free Radical Biology and Medicine*, *63*, 1–29. doi:10.1016/j.freeradbiomed.2013.03.018

Chen, Y., Yang, M., Deng, J., Chen, X., Ye, Y., Zhu, L., … Wu, J. Y. (2011). Expression of human FUS protein in Drosophila leads to progressive neurodegeneration. *Protein & cell*, *2*(6), 477–486. doi:10.1007/s13238-011-1065-7

Cohen, M. S., Orth, C. B., Kim, H. J., Jeon, N. L., & Jaffrey, S. R. (2011). Neurotrophin-mediated dendrite-to-nucleus signaling revealed by microfluidic compartmentalization of dendrites. *Proceedings of the National Academy of Sciences of the United States of America*, *108*(27), 11246–11251. doi:10.1073/pnas.1012401108

Colon-Ramos, D. A. (2009). Synapse Formation in Developing Neural Circuits. In *Current Topics in Developmental Biology* (Vol. 87). Elsevier Inc.

Conte, A., Lattante, S., Zollino, M., Marangi, G., Luigetti, M., Del Grande, A., … Sabatelli, M. (2012). P525L FUS mutation is consistently associated with a severe form of juvenile

amyotrophic lateral sclerosis. *Neuromuscular disorders: NMD*, *22*(1), 73–75. doi:10.1016/j.nmd.2011.08.003

Couthouis, J., Hart, M. P., Erion, R., King, O. D., Diaz, Z., Nakaya, T., … Gitler, A. D. (2012). Evaluating the role of the FUS/TLS-related gene EWSR1 in amyotrophic lateral sclerosis. *Human molecular genetics*, *21*(13), 2899–2911. doi:10.1093/hmg/dds116

Cozzolino, M., & Carrì, M. T. (2012). Mitochondrial dysfunction in ALS. *Progress in Neurobiology*, *97*(2), 54–66. doi:10.1016/j.pneurobio.2011.06.003

Da Cruz, S., & Cleveland, D. W. (2011). Understanding the role of TDP-43 and FUS/TLS in ALS and beyond. *Current opinion in neurobiology*, *21*(6), 904–919. doi:10.1016/j.conb.2011.05.029

Dormann, D., Rodde, R., Edbauer, D., Bentmann, E., Fischer, I., Hruscha, A., … Haass, C. (2010). ALS-associated fused in sarcoma (FUS) mutations disrupt Transportin-mediated nuclear import. *The EMBO Journal*, *29*(16), 2841–2857. doi:10.1038/emboj.2010.143

Fushimi, K., Long, C., Jayaram, N., Chen, X., Li, L., & Wu, J. Y. (2011). Expression of human FUS/TLS in yeast leads to protein aggregation and cytotoxicity, recapitulating key features of FUS proteinopathy. *Protein & cell*, *2*(2), 141–149. doi:10.1007/s13238-011-1014-5

Giordano, G., & Costa, L. G. (2011). Primary Neurons in Culture and Neuronal Cell Lines for In Vitro Neurotoxicological Studies. In L. G. Costa, G. Giordano, & M. Guizzetti (Eds.), *In Vitro Neurotoxicology* (Vol. 758, pp. 13–27). Totowa, NJ: Humana Press. Retrieved from http://www.ncbi.nlm.nih.gov/books/NBK21535/

Hargreaves, I. P. (2003). Ubiquinone: cholesterol's reclusive cousin. *Annals of clinical biochemistry*, *40*(Pt 3), 207–218. doi:10.1258/000456303321610493

Kelso, G. F., Porteous, C. M., Coulter, C. V., Hughes, G., Porteous, W. K., Ledgerwood, E. C., … Murphy, M. P. (2001). Selective targeting of a redox-active ubiquinone to mitochondria within cells: antioxidant and antiapoptotic properties. *The Journal of biological chemistry*, *276*(7), 4588–4596. doi:10.1074/jbc.M009093200

Lagier-Tourenne, C., & Cleveland, D. W. (2009). Rethinking ALS: the FUS about TDP-43. *Cell*, *136*(6), 1001–1004. doi:10.1016/j.cell.2009.03.006

Lanson, N. A., Maltare, A., King, H., Smith, R., Kim, J. H., Taylor, J. P., … Pandey, U. B. (2011). A Drosophila model of FUS-related neurodegeneration reveals genetic interaction between FUS and TDP-43. *Human Molecular Genetics*. doi:10.1093/hmg/ddr150

Lin, M. T., & Beal, M. F. (2006). Mitochondrial dysfunction and oxidative stress in neurodegenerative diseases. *Nature*, *443*(7113), 787–795. doi:10.1038/nature05292

Lodish, H., Berk, A., & Zipursky, S. (2000). Overview of Neuron Structure and Function. In *Molecular Cell Biology* (4th Edition.). New York: W. H. Freeman.

Manfredi, G., & Xu, Z. (2005). Mitochondrial dysfunction and its role in motor neuron degeneration in ALS. *Mitochondrion*, *5*(2), 77–87. doi:10.1016/j.mito.2005.01.002

McManus, M. J., Murphy, M. P., & Franklin, J. L. (2011). The Mitochondria-Targeted Antioxidant MitoQ Prevents Loss of Spatial Memory Retention and Early Neuropathology in a Transgenic Mouse Model of Alzheimer's Disease. *The Journal of Neuroscience*, *31*(44), 15703–15715. doi:10.1523/JNEUROSCI.0552-11.2011

Murakami, T., Yang, S.-P., Xie, L., Kawano, T., Fu, D., Mukai, A., … St George-Hyslop, P. (2012). ALS mutations in FUS cause neuronal dysfunction and death in Caenorhabditis elegans by a dominant gain-of-function mechanism. *Human molecular genetics*, *21*(1), 1–9. doi:10.1093/hmg/ddr417

Murphy, M. P., & Smith, R. A. J. (2007). Targeting antioxidants to mitochondria by conjugation to lipophilic cations. *Annual review of pharmacology and toxicology*, *47*, 629–656. doi:10.1146/annurev.pharmtox.47.120505.105110

Shi, P., Gal, J., Kwinter, D. M., Liu, X., & Zhu, H. (2010). Mitochondrial dysfunction in amyotrophic lateral sclerosis. *Biochimica et Biophysica Acta (BBA) - Molecular Basis of Disease*, *1802*(1), 45–51. doi:10.1016/j.bbadis.2009.08.012

Tauskela, J. S. (2007). MitoQ--a mitochondria-targeted antioxidant. *IDrugs: the investigational drugs journal*, *10*(6), 399–412.

Tradewell, M. L., Yu, Z., Tibshirani, M., Boulanger, M.-C., Durham, H. D., & Richard, S. (2012). Arginine methylation by PRMT1 regulates nuclear-cytoplasmic localization and toxicity of FUS/TLS harbouring ALS-linked mutations. *Human molecular genetics*, *21*(1), 136–149. doi:10.1093/hmg/ddr448

Ugras, S. E., & Shorter, J. (2012). RNA-Binding Proteins in Amyotrophic Lateral Sclerosis and Neurodegeneration. *Neurology research international*, *2012*, 432780. doi:10.1155/2012/432780

Wang, J., Ren, L., Li, L., Liu, W., Zhou, J., Yu, W., … Chen, S. (2009). Microfluidics: a new cosset for neurobiology. *Lab on a chip*, *9*(5), 644–652. doi:10.1039/b813495b

Xia, R., Liu, Y., Yang, L., Gal, J., Zhu, H., & Jia, J. (2012). Motor neuron apoptosis and neuromuscular junction perturbation are prominent features in a Drosophila model of Fus-mediated ALS. *Molecular Neurodegeneration*, *7*, 10. doi:10.1186/1750-1326-7-10

Acknowledgements

There are several people who played a significant role in making this investigation possible. First of all, I would like to thank Dr. Jane Wu, the Charles Louis Mix Professor of Neurology and my advisor at the Feinberg School Medicine, for allowing me to conduct research in her lab. She provided invaluable support throughout the investigation and shared useful advice and information with me. Additionally, I would like to thank Mengmeng Chen, my mentor, for providing constant guidance and instruction throughout the process. She assisted me with finding background information, instructed me in a variety of laboratory techniques, and worked closely with me in many aspects of my project. I would also like to acknowledge the help of Xiaoping Chen, a research associate in the lab, for helping out with so many different tasks around the lab and making everyone's research possible. Finally, I would like to thank Dr. Judith Scheppler and the rest of the SIR staff at IMSA for giving me the opportunity to conduct research.

Appendix

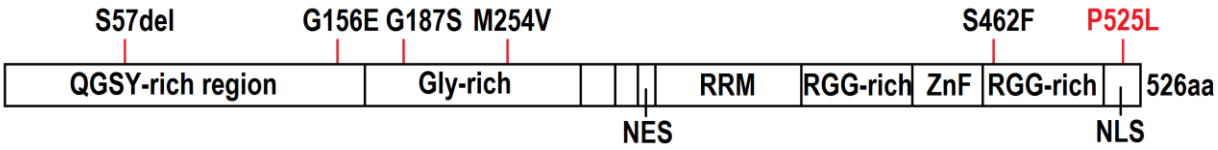

Figure 1. A gene map of the FUS/TLS gene. The P525L mutation is designated in red font.

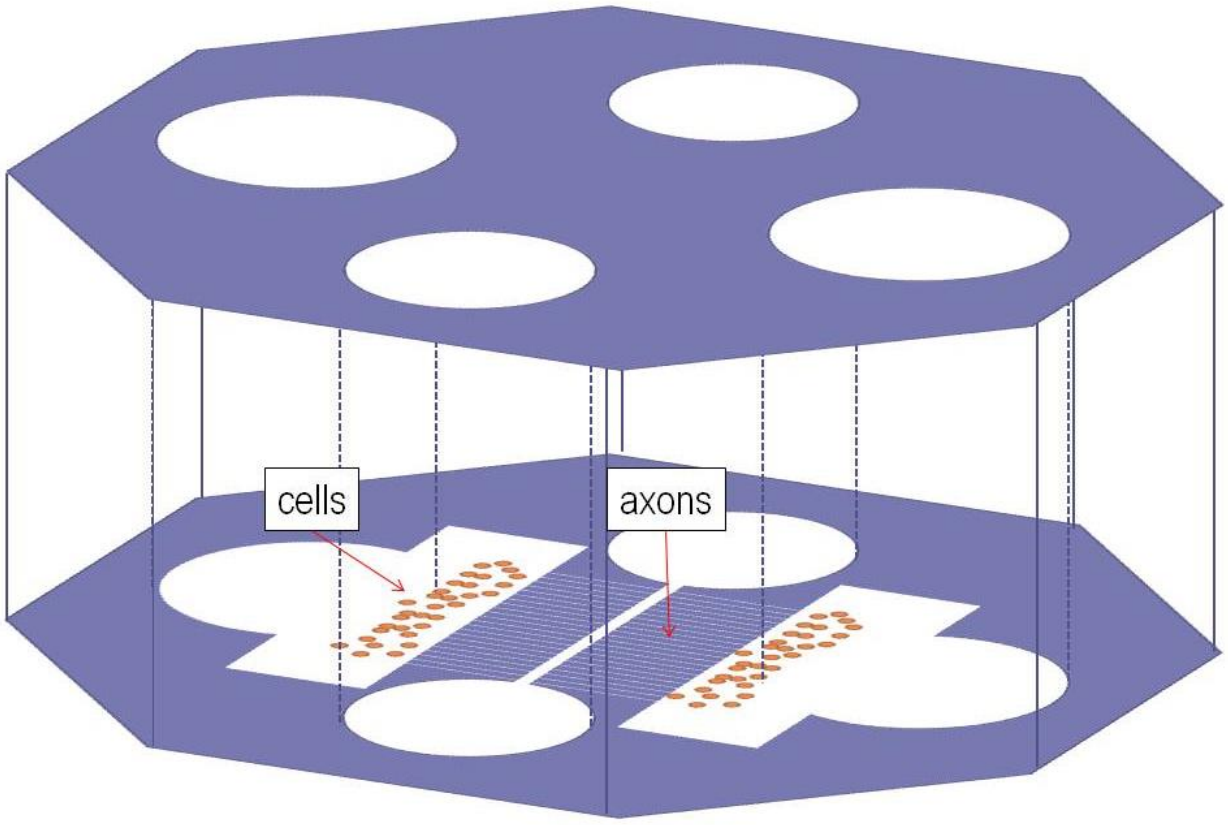

Figure 2. The microfluidic chamber design. The chamber is made of polydimethylsiloxane (PDMS) and is 14 mm in diameter, fitting in one well of a 12-well microtiter plate. Neurons are plated in the two opposite large holes, and axons are allowed to grow in straight lines through the microgrooves.

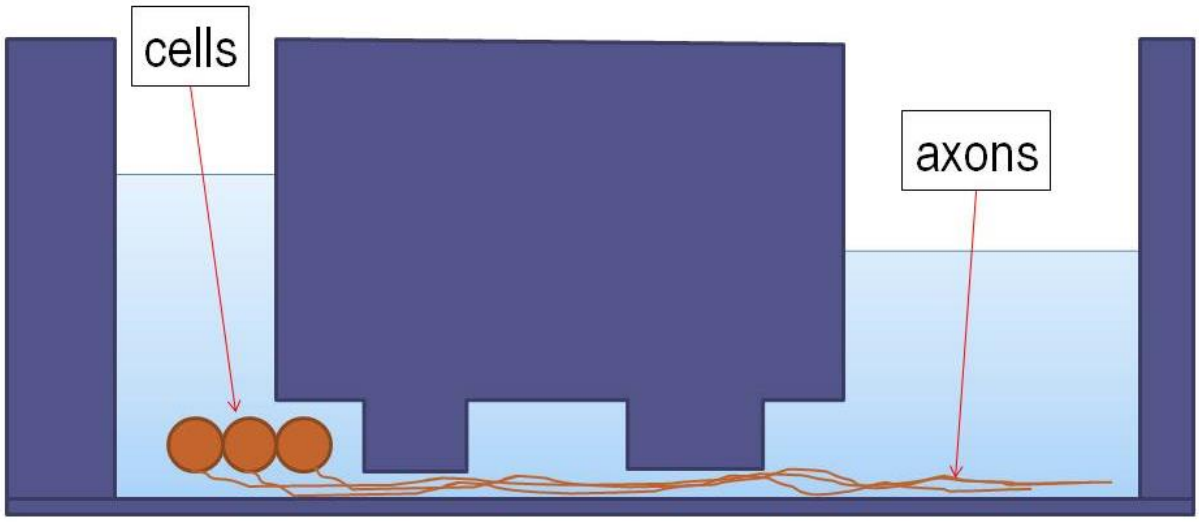

Figure 3. Detailed cross-section of one microgroove of a microfluidic chamber. The cells are plated in the large holes, and the microgrooves are only large enough for axons to grow through. Cells can also be plated in both holes, allowing synapses to form in the center area.

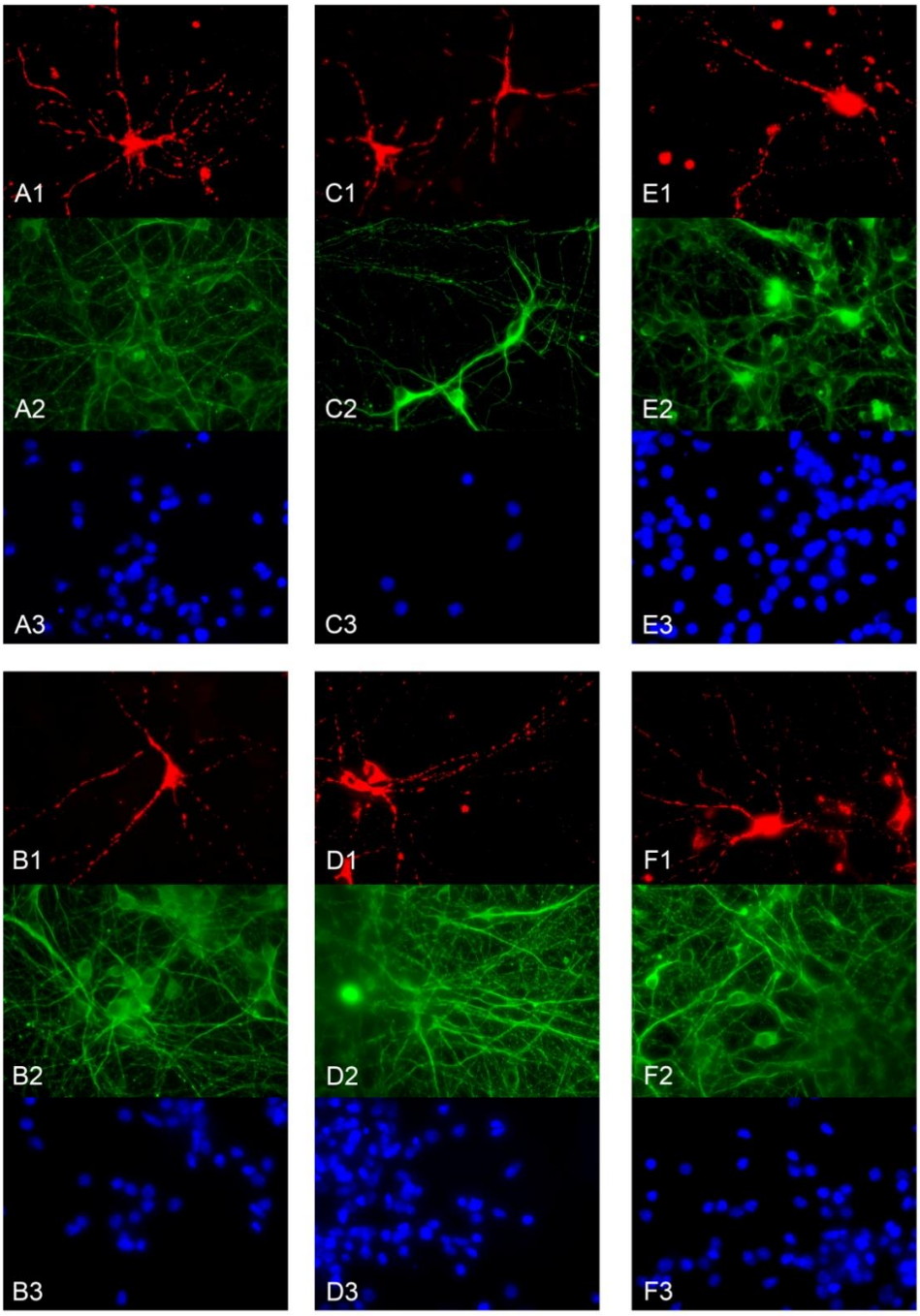

Figure 4.Images depicting mitochondrial fragmentation in neuronal cells. Neurons were transfected with three different plasmids and treated with 0.1 µM MitoQ or no MitoQ. Images were taken using a fluorescent microscope. A: Control transfection, no MitoQ. B: Control transfection, 0.1 µM MitoQ. C: Wild-type FUS transfection, no MitoQ. D: Wild-type FUS transfection, 0.1 µM MitoQ. E: P525L mutant FUS transfection, no MitoQ. F: P525L mutant FUS transfection, 0.1 µM MitoQ. Images 1-3 depict the same region; Image 1: Cy3 channel, Image 2: FITC channel, Image 3: DAPI channel.

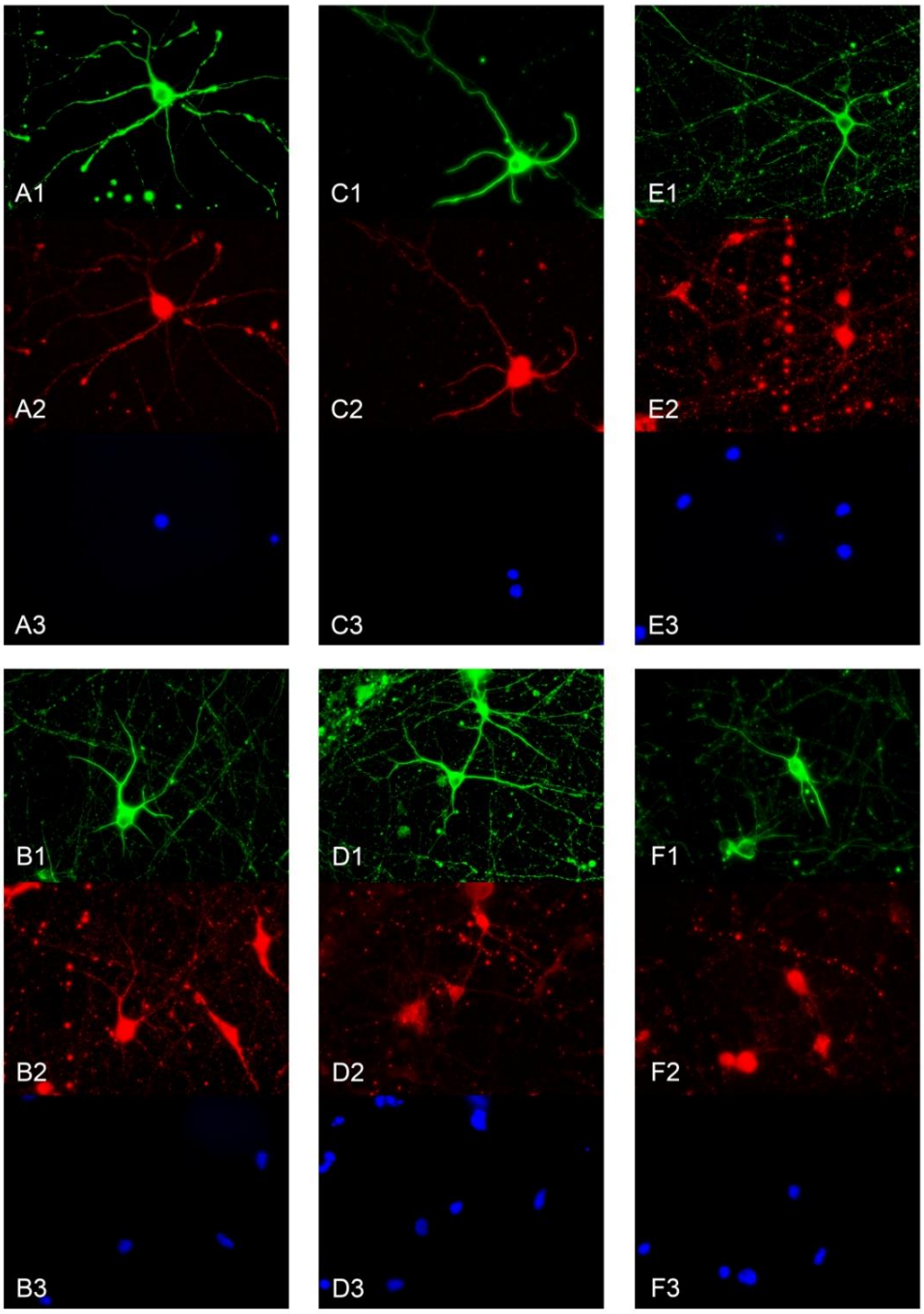

Figure 5. Images depicting dendrites of neuronal cells. Neurons were transfected with three different plasmids and treated with 0.1 µM MitoQ or no MitoQ. Images were taken using a fluorescent microscope. A: Control transfection, no MitoQ. B: Control transfection, 0.1 µM MitoQ. C: Wild-type FUS transfection, no MitoQ. D: Wild-type FUS transfection, 0.1 µM MitoQ. E: P525L mutant FUS transfection, no MitoQ. F: P525L mutant FUS transfection, 0.1 µM MitoQ. Images 1-3 depict the same region; Image 1: FITC channel, Image 2: Cy3 channel, Image 3: DAPI channel.

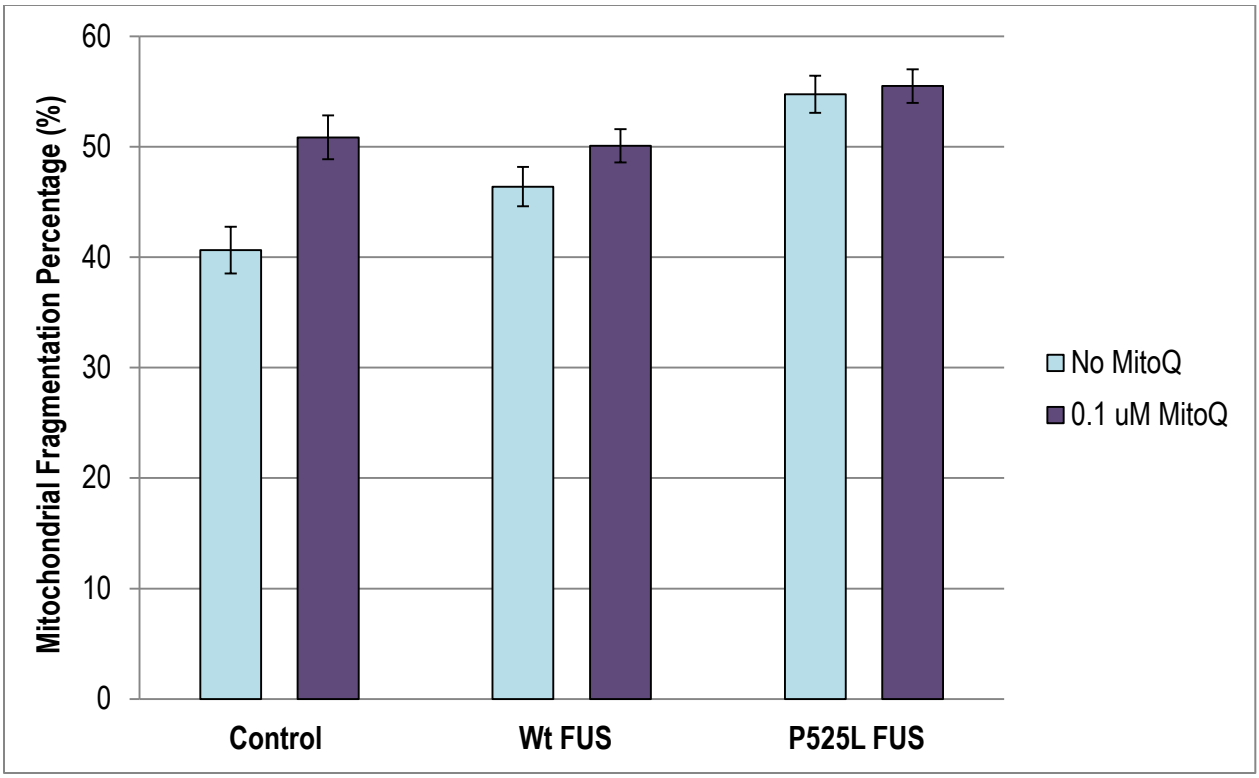

Figure 5. Mitochondrial fragmentation percentage in neurons treated with MitoQ. Mitochondrial fragmentation percentage was evaluated for each 30 µm segment of each dendrite, based on the percentage of length not covered by mitochondria. The data was graphed with error bars with one standard error above and below the mean. Neurons were transfected with control, wild-type FUS, and P525L mutant FUS plasmids prior to drug treatment. MitoQ treatment significantly worsened mitochondrial fragmentation, and fragmentation was significantly increased from the control transfection to the wild-type FUS and P525L mutant FUS transfections.

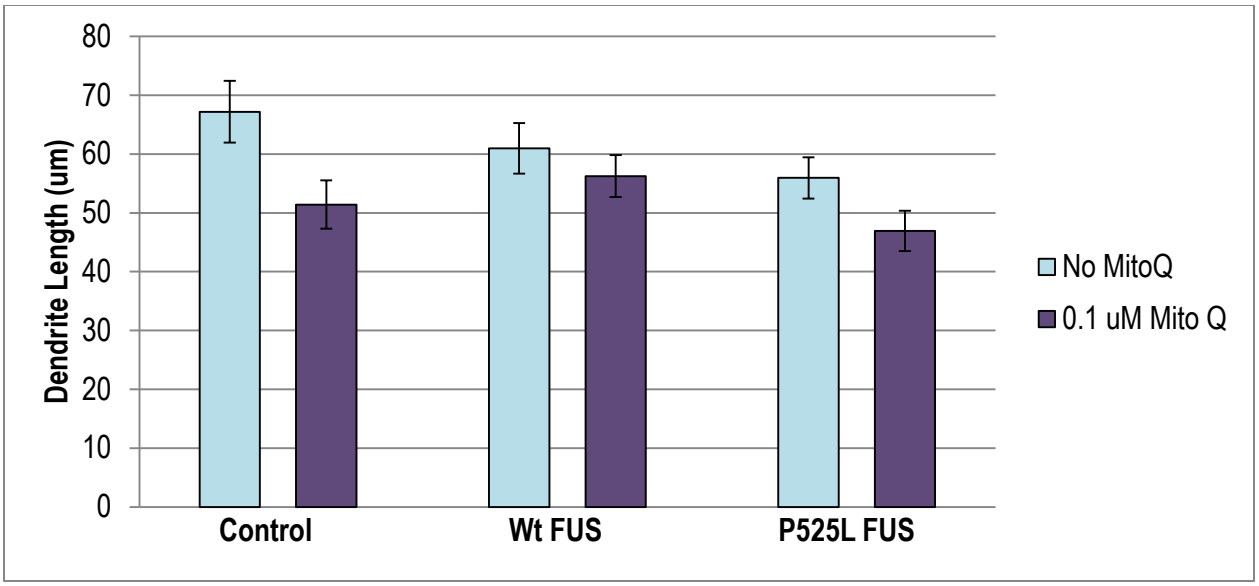

Figure 6. Dendrite length in neurons treated with MitoQ. Dendrite length was measured in µm from the cell body to the end of the dendrite. Each dendrite was measured separately, and each resulting dendrite from each branch point was also measured separately. The data was graphed with error bars one standard error above and below the mean. Neurons were transfected with control, wild-type FUS, and P525L mutant FUS plasmids prior to drug treatment. MitoQ treatment was found to significantly decrease the dendrite length

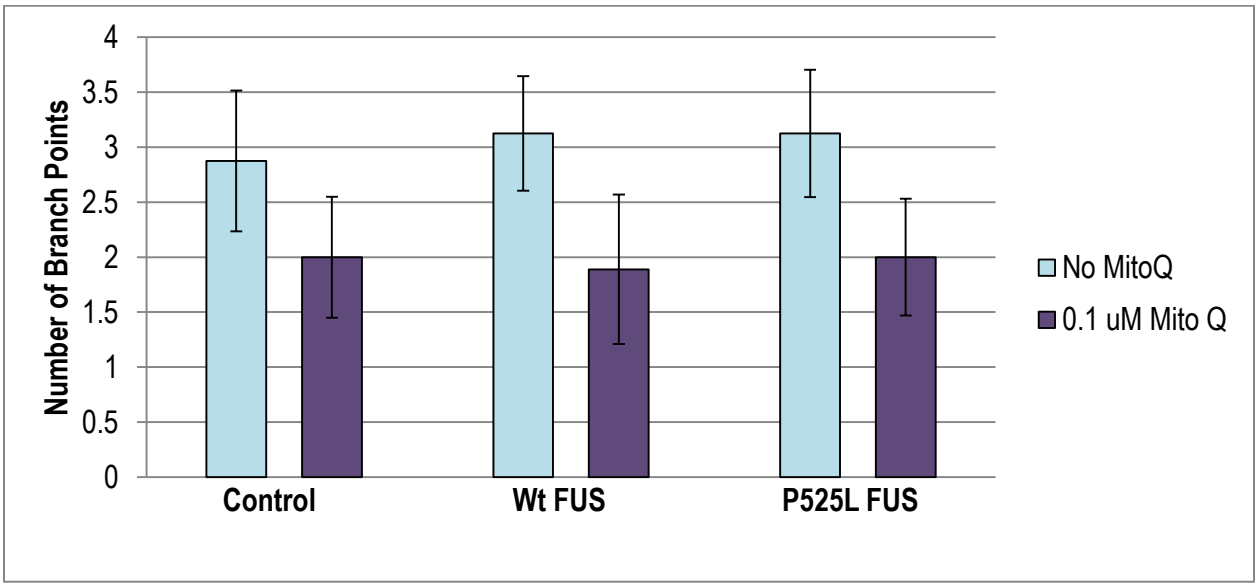

Figure 7. Number of branch points per neuron in neurons treated with MitoQ. A branch point was defined as a point at which a single dendrite split into two dendrites, and the total number of branch points was counted for each neuron. The average number of branch points per neuron was graphed with error bars depicting one standard error above and below. Neurons were transfected with control, wild-type FUS, and P525L mutant FUS plasmids prior to drug treatment. MitoQ treatment significantly decreased the average number of branch points per neuron.

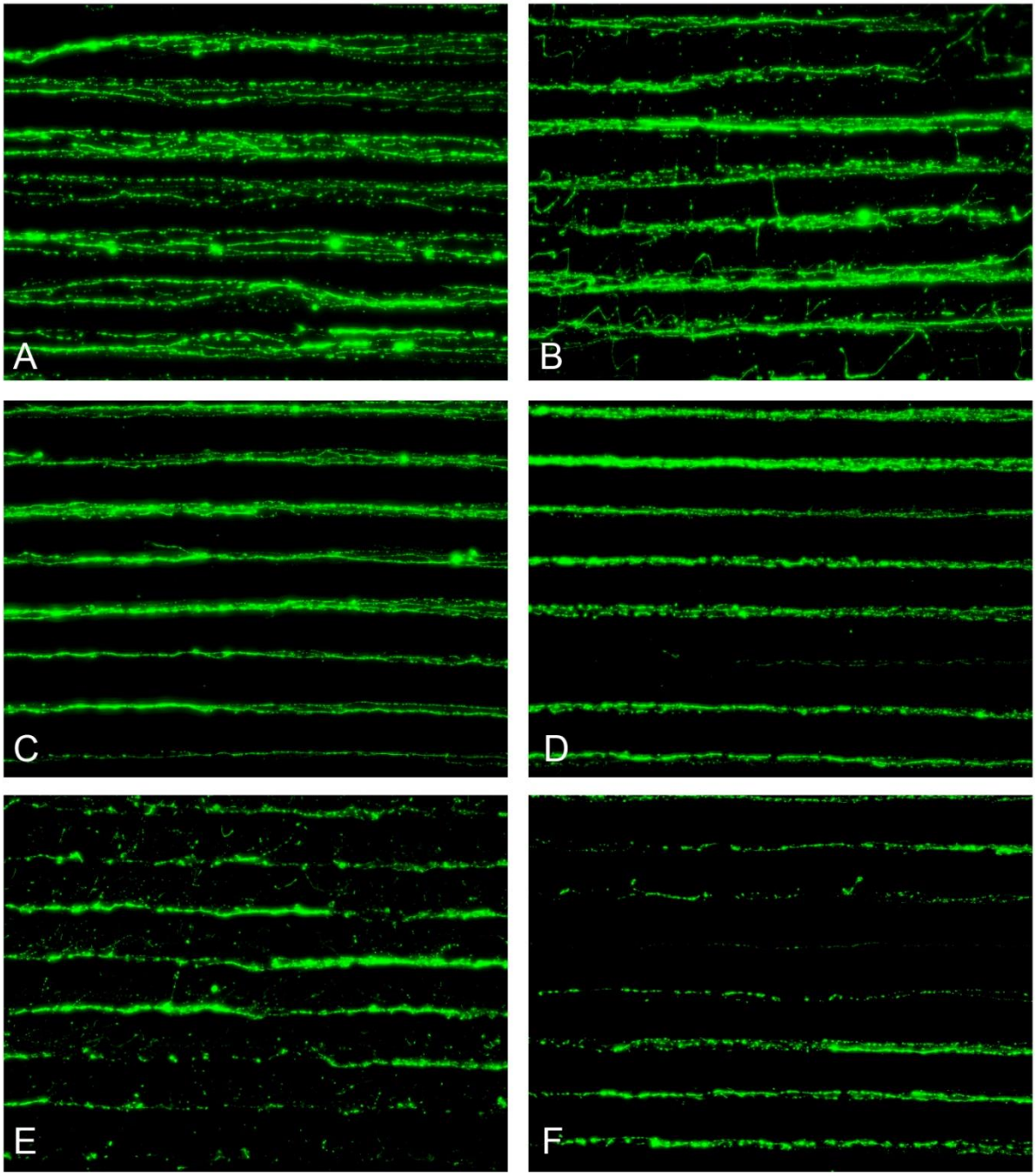

Figure 9.Axons grown in the microgrooves of a microfluidic chamber, imaged using the FITC channel of a fluorescent microscope. Neurons were transfected with three different plasmids and treated with 0.1 µM MitoQ or no MitoQ. A: Control transfection, no MitoQ. B: Control transfection, 0.1 µM MitoQ. C: Wild-type FUS transfection, no MitoQ. D: Wild-type FUS transfection, 0.1 µM MitoQ. E: P525L mutant FUS transfection, no MitoQ. F: P525L mutant FUS transfection, 0.1 µM MitoQ. MitoQ treatment negatively affected the fragmentation and growth of axons.